Development and Characterization of a 2-D microchip-based Protein separation system.

J.J. Feng[2*], V Olazábal[1*], J.A. Olivares[1], S. Sundaram[2], S. Krishnamoorthy[2] & S. Iyer[1]

[1]B-4, Bioscience Division, Los Alamos National Laboratory, Los Alamos, NM 87545
[2]CFD Research Corporation, 215 Wynn Drive, Huntsville, Alabama 35805, USA
* these authors contributed equally
Correspondence to: siyer@lanl.gov and sk@cfdrc.com

ABSTRACT

We have developed a 2-D microchip based separation system that employs capillary isoelectric focusing (CIEF) coupled with capillary zone electrophoresis (CZE) and uses a real-time fluorescent imaging of the analytes as they are separated. Physics-based simulations have been developed to understand the fundamental physico-chemical processes occurring in this system. Here, we describe the design of the chip, instrument and detection system, characterize the operation and present results from preliminary simulations to understand and establish optimal separation conditions.

Keywords: capillary isoelectric focusing, capillary zone electrophoresis, chip, laser-induced fluorescence, and simulation.

1 INTRODUCTION

Traditional methods in proteomics have relied on gel-based separation of proteins followed by directed cleavage of these proteins and mass spectrometry to measure the products [1,2]. The emphasis on reliable, high-throughput analyses has led to the development of novel "pre-mass spec" separation approaches such as multidimensional liquid-chromatography (LC) of tryptic peptides [3]. While an effective technique, comparable expression levels cannot be determined using this approach unless some form of labeling is employed. Hence there is need for approaches that can suitably compare the effects of experimental treatment on intact proteins prior to peptide generation. The ideal separation system would allow real time imaging of the separation, use a labeling system that would enable a wide dynamic range of detection and facilitate interfacing with downstream procedures, such as mass spectrometry. To this end, we have developed a 2-D separation chip-based system, similar to that reported in [4], that employs capillary isoelectric focusing (CIEF) coupled with capillary zone electrophoresis (CZE) but uses real-time fluorescent imaging of the proteins over the whole separation area.

Design and development of such a system is a relatively complicated task. One needs to understand the fundamental physico-chemical processes, such as fluid flow, electric field and mass transport, occurring in this system before making any design changes. In this regard, physics-based simulations can play a vital role. Here we present the results of our preliminary simulations performed to characterize the separation conditions. Detailed models for the transport of protein mixtures in both porous and non-porous medium with associated electrokinetic phenomenon are under development. While, validation and design optimization of the 2D separation device using these models will be reported in a future communication, separations in individual dimensions were performed using a scanning LIF CE for cIEF [5] and a Beckman MDQ for CZE (data not shown) in gel filled media using neutral capillaries. Separation buffers and conditions were as per the manufacturer's instructions.

2 2-D SEPARATION SYSTEM

2-D Chip. A schematic of the 2-D chip is shown in Figure 1. The chip employs capillary isoelectric focusing (CIEF) in the first dimension coupled with capillary zone electrophoresis (CZE) in the second dimension. In this configuration, IEF separates proteins based on their isoelectric point. A fraction from the first capillary is transferred to a second capillary, where the contents are separated based on their size. In this fashion, the entire sample is subjected to two-dimensional separation.

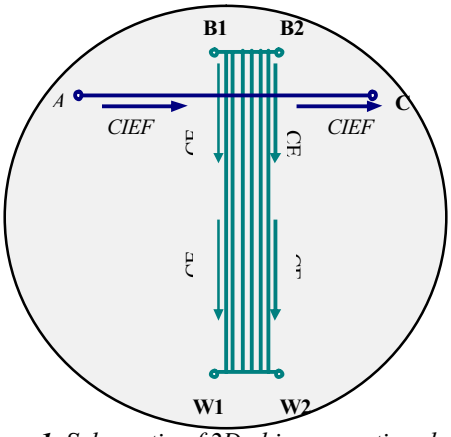

Figure 1. *Schematic of 2D chip separation device. Reservoir A: Anolyte, Reservoir C: Catholyte, Reservoir B1 and B2: Buffer and Reservoir W1 and W2: Waste*

This glass planar chip was designed in-house and fabricated by Motorola using standard photolithographic techniques and chemical wet etching [6]. It is placed in a holder with fluid reservoirs for loading sample, and where several platinum electrodes allow connection to the power supply.

Laser-induced fluorescence detection system (LIF). The laser-induced fluorescence detection system is shown in Figure 2. An epi-illumination configuration is used for the LIF detection. Light from a fiber-optic coupled argon ion laser, 488-nm emission line, is directed by a dichroic filter through lenses onto the 2-D chip surface. Emitted light passes through the dichroic, a bandpass, and a Holographic SuperNotch-Plus filter, and is focused onto a photomultiplier tube. The 2-D chip separation device is held in a stepper motor X-Y translation table. A Visual Basic program controls the X-Y table and acquires the photomultiplier output data from a 12-bit ADC board.

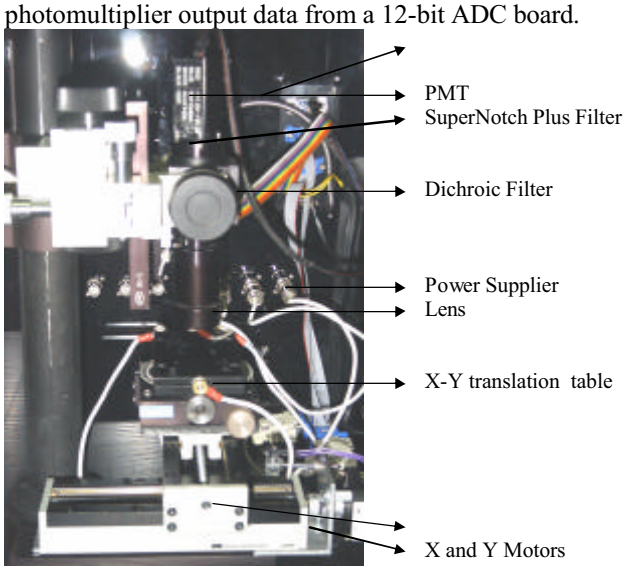

Figure 2. *Laser-Induced fluorescence detection system for the 2-D.*

In order to design and develop an optimal and highly efficient separation system, the following design issues need to be addressed:

- What effect do gels have on separation?
- What are the optimal device dimensions to accomplish separation with minimal dispersion?
- How to generate required pH gradients within given space constraints of the CIEF channel and yet cover the range of pI points?
- What is the effect of geometry on leakage of buffer or current at CIEF-CZE channel intersection?

Multiphysics simulation of the combined CIEF-CZE phenomena can help answer the above questions. In this regard, an electrokinetic transport model in porous media has been implemented in CFD-ACE+[7], a commercial multiphysics simulation software developed and marketed by CFD Research Corporation. This, in conjunction with other electrokinetic transport models reported earlier [8], is used in the preliminary design analysis.

3 SIMULATION OF 2D SEPARATION

Simulation of 2D separation process is extremely complex due to nonlinear interactions among fluid flow, electric field, and sample transport. Full sets of governing nonlinear equations need to be solved. Besides, the presence of porous (gel) material in these systems will introduce additional complexities. In general the gel can be modeled as fibrous porous material that allows species smaller than the characteristic pore diameter to move through. The models developed are based on "effective medium approach" in which the effects of gel on flow, electric field and species transport are accounted for by introducing apparent parameters such as hydrodynamic permeability, effective electrical conductivity, hindered diffusion coefficient, and reduced electrophoretic mobility. Simulations that model hydrodynamic and transport processes at scales comparable to pore dimension, accounting for fiber orientation are infeasible. The governing equations are briefly summarized below.

Fluid mass Conservation:

$$\frac{\partial \varepsilon \rho}{\partial t} + \nabla \cdot \varepsilon \rho \mathbf{U} = 0 \qquad (1)$$

Momentum Conservation:

$$\frac{\partial \varepsilon \rho \mathbf{U}}{\partial t} + \nabla \cdot \varepsilon \rho \mathbf{U}\mathbf{U} = -\varepsilon \nabla p + \nabla \cdot \varepsilon \mathbf{t} + \varepsilon \mathbf{B} - \frac{\mu \varepsilon^2}{k_p}\mathbf{U} \qquad (2)$$

Analyte conservation:

$$\frac{\partial \varepsilon \rho c_i}{\partial t} + \nabla \cdot \mathbf{J} = R_i \qquad (3)$$

in which the flux is given by Nernst-Planck equation

$$\mathbf{J}_i = \varepsilon \rho U c_i - \rho D_{i,eff} \nabla c_i + z_i c_i \omega_{i,eff} \nabla \phi \qquad (4)$$

Conservation of Electric Current:

$$\nabla \cdot \sigma_{eff} \nabla \phi = 0 \qquad (5)$$

Here ε is porosity of the fibrous medium and the other symbols are self-explanatory.

Of particular importance, the hindered diffusivity is calculated from [9]

$$\frac{D_{eff}}{D_0} = \left[1 + \frac{a}{\sqrt{k_p}} + \frac{a^2}{k_p^2}\right]^{-1} S(f), f = \left(1 + \frac{a}{R_s}\right)^2 (1-\varepsilon) \qquad (6)$$

where a is species radius, R_s is the fiber radius and the steric exclusion is calculated as:

$$S = \frac{1}{1-f}\left[1 - 2f\left(1 + f - \frac{0.306 f^4}{1 - 1.403 f^8} - 0.0134 f^8\right)^{-1}\right]$$

The electrophoretic mobility in gel is calculated based on Slater's model [10]

$$\frac{\omega_{eff}}{\omega_0} = \frac{1}{2-\varepsilon}, 0.5 < \varepsilon < 1 \qquad (7)$$

for ordered fiber matrix and

$$\frac{\omega_{eff}}{\omega_0} = \frac{1}{3} + \frac{2}{3}\varepsilon, 0.5 < \varepsilon < 1 \qquad (8)$$

for a random fiber matrix. Table 1 summarizes models used in calculated apparent parameters:

Table 1: Summary of Effective Medium Models

Parameter	Model
Permeability k_p	Unit cell model [11,12]
Hindered Diffusivity D_{eff}	Brady's model [9]
Electrophoretic Mobility ω_{eff}	Slater's model [10]
Electric Conductivity σ_{eff}	Unit cell model [13]

The governing equations (1-5) are solved by an implicit finite-volume numerical scheme [7,8].

4 RESULTS AND DISCUSSIONS

The preliminary simulations are performed to analyze the impact of porosity of the gel matrix on sample separation and dispersion. Both separation (vertical) and IEF (horizontal) channels are assumed to be filled with gel matrix of porosity ε_1 and ε_2, respectively. In the first set of simulations, ε_1 was kept at a constant value of 0.9, while ε_2 was varied from 0.5 to 1.0.

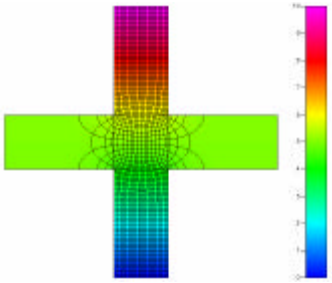

Figure 3. Potential and Field at Channel Junction

Electric field of 200 V/cm is applied in the separation channel, while IEF channel is floated. Governing equations (1-5) are solved satisfying appropriate boundary conditions. Figure 3 shows a contour plot of electric potential and iso-electric field lines. Significant distortion in the field is observed near channel intersection, which could be attributed to the fanning (leakage) effect.

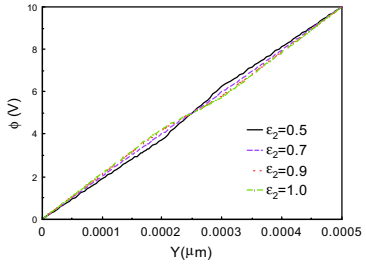

Figure 4. Potential Distribution Along the Separation Channel Various ε_2.

Figure 4 illustrates, variations in the electric potential along the axis of the separation channel as a function of porosity of gel in the IEF channel. The resulting electric potential is linear in the separation channel except near the junction of IEF and separation channels where distortions are observed due to the discontinuity in the gel porosity. The distortion in the contour lines is maximum for $\varepsilon_2 = 0.5$. The variations in the electric field strength in the separation channel, as well as in the center of the intersection are shown in Figure 5. As expected, only small variations are observed in the separation channel (which will ultimately vanish at locations far from intersection). However, the electric field strength increases with decrease in ε_2 since the fibers are assumed non-conductive and total current is conserved in the mathematical formulation. Changes in the field strength are attributed to both leakage current and changes in the area available for current conduction.

Next, the results from a sample separation study in gel and a non-gel media are presented. The purpose of this study is to understand the effect of gel matrix on separation and sample dispersion. The properties of species used in the simulation are listed in Table 2. The hydrodynamic permeability is assumed to be 1E11m^2. The fiber spacing is calculated from given porosity. Brady's model for diffusion coefficient and Slater's model for electrophoresis mobility, both valid for random oriented fibrous gel, are used. An electric field of 100 V/cm is applied to the separation channel. The detection point on the separation channel is located at 3cm from the intersection of CIEF and CZE channels.

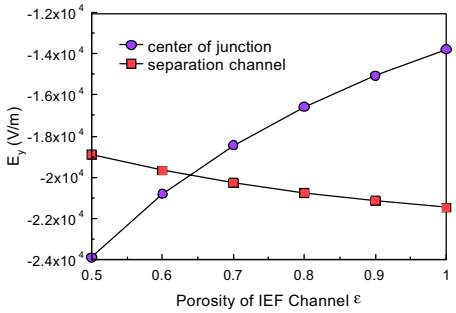

Figure 5. Electric Field at Separation Channel and At Channel Intersection for Various Porosities of IEF Gel.

Table 2: Species Properties

Species	Glutamic Acid	Histidine
Diffusivity (m^2/s)	7.45E-10	7.316E-10
Mobility (m^2/s/V)	2.9E-8	2.25E-8
Init. Conc. (μM)	1.0	1.5

Figure 6 shows an electropherogram predicted by the simulation at the detection point. The first plot shows concentration of glutamic acid and histidine when the separation channel is filled with the buffer solution only. In the second plot, concentration levels are shown when the separation channel is filled with a gel medium of porosity of 0.9. It is observed that both species are dispersed (largely due to molecular diffusion) as they move along the channel. The peak concentration is about 6% of their initial values. Also observed are time lags between the signals of the same species when it is run in the channel with and without a gel medium. This is attributed to hindered diffusion and reduced electrophoretic mobility due to the presence of gel medium. The signal peaks at the observation point are delayed by 7 and 8 seconds, respectively, for glutamic acid and histidine. These delays are approximately (inversely) proportional to reduced liquid

volume fraction due to the presence of gel. On the other hand, it is also interesting to note that the dispersion of the sample profile is reduced (reduced band broadening) especially during the short separation time. This is illustrated in Figure 7 where concentration contour plots for glutamic acid and histidine are shown at T=80s after separation field is applied. This figure indicates that the species are focused into a tighter band due to the presence of porous medium, when compared with the situation when the channels are filled with only non-porous buffer solution.

5 CONCLUSIONS

Separation of species in a capillary electrophoretic system has been analyzed using computational models. Effective media approach based methodology has been implemented, where the transport coefficients and other parameters are computed using porosity-based "unit-cell" models. Computational tools have been applied to understand the influence of gel medium on electrophoretic separation of species. Preliminary results indicate that though the gel medium affected the transport (delay in peak signal), reduced band broadening was also observed due to reduced diffusion coefficient. Further model development is required that will account for transport of protein mixture coupled with ionization, biochemical reactions under the influence of electroosmotic flow in porous matrix. Development of these models, validation and design optimization of the 2D separation device are under progress and will be reported later.

ACKNOWLEDGEMENT

JJF, SK and SS acknowledge CFD Research Corporation for internal research support. VO, JO, SI acknowledge financial support from the LANL LDRD program. Los Alamos National Laboratory is operated by the University of California for the U.S. Department of Energy under contract no. W-7406-ENG-36.

REFERENCES

1. S-E, Ong, and A. Pandey, Biomol. Eng. 18, 195, 2001.
2. S. Beranova-Giorgianni. Trends Ana. Chem., 22, 273, 2003.
3. D.A. Wolters, M.P. Washburn. J.R. Yates, Anal. Chem. 73, 5683, 2001.
4. A.E. Herr, J.I. Molho, K.A. Drouvalaski, J.C. Mikkelsen, P.J. Utz, J.G. Santiago, and T.W. Kenny. Anal. Chem. 75, 1180, 2003.
5. JA Olivares, PC Stark, P Jackson. Anal Chem. 2002 May 1;74(9):2008-13.
6. C.S. Effenhauser, A. Manz, and H.M. Widmer, Anal. Chem. 65, 2637, 1993.
7. Anonymous, *CFD-ACE+ Users Manual*, CFD Research Corporation, Huntsville, AL, 2003.
8. Krishnamoorthy, J. J. Feng, and V. B. Makhijani, "Analysis of Sample Transport in Capillary Electrophoresis Microchip Using Full-Scale Numerical Analysis", *Proc. 4th Int. Conf. on Modeling and Simulation of Microsystems*, Hilton Head, SC, 2001.\
9. E. Johnson et. al., 1996 "Hindered Diffusion in Agarose Gels: Test of Effective Medium Model", *Biophy. J.* **70**, 1071.
10. J. Mercier & G. W. Slater 2001 "An Exactly Solvable Ogston Model of Gel Electrophoresis. 7. Diffusion and Mobility of Hard Spherical Particles in Three-Dimensional Gels", *Macromolecules*, **34**, 3437.
11. J. Happel 1959 "Viscous Flow Relative to Arrays of Cylinders", *AIChE J*, **5**, 174.
12. G. W. Jackson & D. F. James 1986 "The Permeability of Fibrous Porous Media", *Can. J. Chem. Eng*. **64**, 264.
13. J. Feng etc. "The Electric Conductivity of Fibrous Porous Media", To be published.

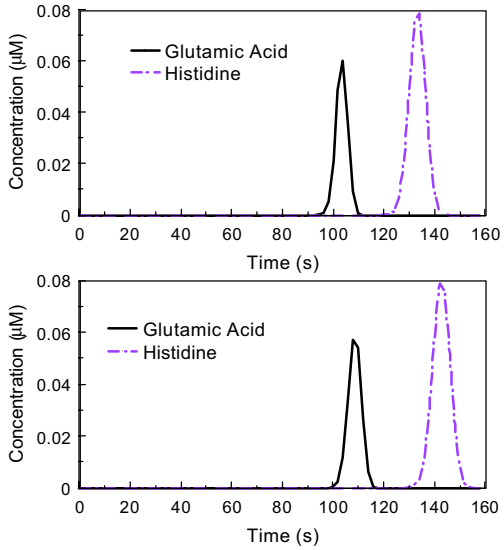

Figure 6. Electropherogram of Separation Without (top) and With Gel (bottom) in the Separation Channel

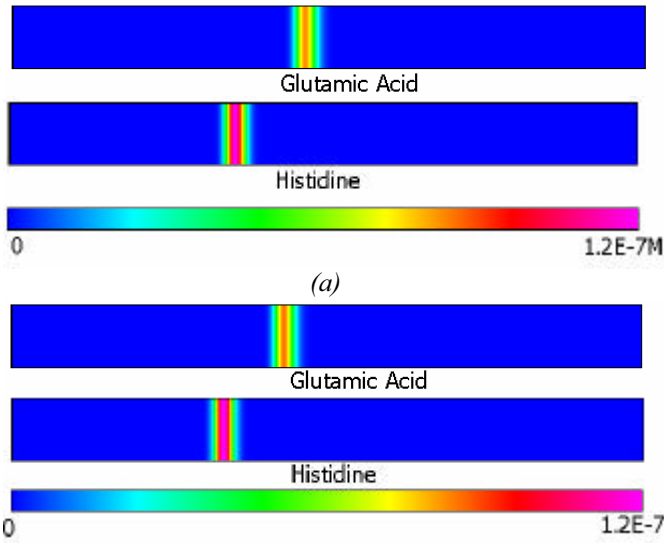

Figure 7. Comparison of Band Broadening in the (a) non-gel and (b) gel-based Medium at T=80s.